

Motion Navigation using Non-Linear Gradient Fields

Emre Kopanoglu¹, Gigi Galiana¹, and Robert Todd Constable¹

¹*Diagnostic Radiology, Yale University, New Haven, Connecticut, United States*

Target Audience: Researchers with an interest in motion tracking or nonlinear gradient fields.

Purpose: Nonlinear gradient fields (NLGFs) vary along at least two directions. Thus, a simple trapezoidal waveform using NLGFs encodes data along at least two dimensions. Supported with a receive-array RF coil, such an acquisition may be used to form low-resolution 2D/3D images for motion navigation. In this study, we demonstrate this approach using a Z2-harmonic ($z^2 - x^2/2 - y^2/2$) and an 8-channel head coil.

Methods: Simulations were performed using Matlab (Mathworks Inc., Natick, MA, USA) with a spatial resolution of 256^2 and an FOV of $(20\text{ cm})^2$. The duration of the motion encoding gradient was 2.56 ms, its amplitude 4 mT/m² and the number of navigator samples 128. Samples were acquired during ramp-up and ramp-down, with the flat-top of the trapezoidal waveform being 1.36 ms. In the simulations, the experimentally obtained sensitivity maps of an 8-channel receiver coil (Figure 1) were used¹. The proposed imaging sequence, used NLGF and a representative voxel distribution are illustrated in Figure 1. The spatial encoding functions generated by the gradient fields were averaged on a 16×16 higher resolution grid (sufficient at the field strength used) to incorporate intra-voxel dephasing.

Motion was assumed to be sinusoidal with some randomness imposed (Figure 2) for simplicity. Each TR ($TR\#i$) was simulated as follows: the target image was translated / rotated; image data were acquired using the coil sensitivities and the Fourier Transform after which the corresponding line in the k-space was selected and stored (ACQ_{im}^i); navigator data were acquired using the spatial-encoding function generated by the NLGF and the coil sensitivities (ACQ_{mot}^i). 2D Motion navigator images were reconstructed using Kaczmarz algorithm with 15 iterations and $\lambda = 0.25$. The first navigator image was set as reference. All succeeding images were translated and rotated in a predefined range of values, and their complex inner product with the reference image was calculated. The translation & rotation values that yielded the magnitude-wise maximum inner-product were stored ($\Delta_x^i, \Delta_y^i, \Delta_\phi^i$). Object images were reconstructed by taking the inverse Fourier Transform of the stored k-space line (ACQ_{im}^i), and translating/rotating the resulting spatial pattern by ($\Delta_x^i, \Delta_y^i, \Delta_\phi^i$) before adding it to the reconstructed image.

Because a nonlinear field and multiple receive coils were used, reconstructed images had noticeable central-brightening. This central brightening does not inhibit motion tracking but dampens the estimated values in a linear fashion. Hence, the motion pattern is well-recovered but scaled. To correct this, the estimated motion is scaled in a range of values, images were reconstructed for each scaling and the sharpest image was selected using the gradient of the image along both transverse dimensions as a measure of sharpness. We would like to stress here that, the images given in Figure 2 are generated by a fully-automated algorithm that includes all the steps, and has neither any user-input nor any knowledge on the shape of the motion or the target image.

Results: Figure 2 shows the estimated motion, and the motion-corrected images for translational motion along x and y , and rotation around z axes in axial images. Average estimation error is below 0.17 mm (0.22 pixels) for translational and 0.4 degrees for rotational motion.

Discussion: For this proof-of-concept study, the motion navigator waveform was not time-optimized and relatively low gradient amplitude and sampling rate were used. By adjusting the NLGF amplitude such that field strength and field rate-of-change are same inside the FOV as those of the linear gradient fields typically available clinically (40 mT/m, 140 T/m/sec), and using the maximum available sampling rate, the duration of the navigator can be reduced to approximately 250 μ s. If the navigator is placed before the data acquisition, then multiple echo sequences are possible, with only a 500 μ s increase in echo-time including rewinding. If used after data acquisition, the method requires rewinding the phase and readout gradient moments.

In its current state, the proposed method can track in-slice translational and rotational rigid body motion. However, because data-acquisition with the NLGF represents a projection imaging sequence, the center of k-space is acquired in each TR. Hence, the presence of through-plane motion can be estimated similar to PROPELLER². Furthermore, because the field varies in all three dimensions, it may track and correct through-plane motion and rotation around x and y axes in slab-imaging cases, using an RF coil-array with separate elements along z .

Fourier Shift Theorem based methods assume that the object and the coil sensitivities do not change due to motion, which necessitates that the coils move with the object³. The proposed method does not have this requirement; to demonstrate this, the method was demonstrated for a case with stationary coils.

One of the advantages of this approach is that it can be seamlessly integrated with the accelerated-acquisition method O-Space imaging⁴ with the pre-phasing waveform before readout.

Conclusion: In this study, a novel motion navigation method that uses RF receiver arrays and nonlinear gradient fields is proposed. As demonstrated, the method can track rigid in-slice translational and rotational motion with sub-pixel precision, whereas tracking of through-plane motion is currently under investigation.

Acknowledgments: NIH R01-EB016978 & R01-EB012289. **References:** 1. Walsh DO *et al.* MRM 2000;43(5):682-690. 2. Pipe JG. MRM 1999;42(5):963-969. 3. Bookwalter CA *et al.* IEEE MI 2010;29(2):339-349. 4. Stockmann JP *et al.* MRM 2010;64(2):447-456.

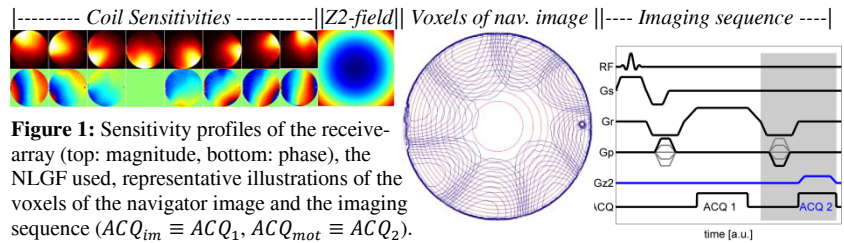


Figure 1: Sensitivity profiles of the receive-array (top: magnitude, bottom: phase), the NLGF used, representative illustrations of the voxels of the navigator image and the imaging sequence ($ACQ_{im} \equiv ACQ_1$, $ACQ_{mot} \equiv ACQ_2$).

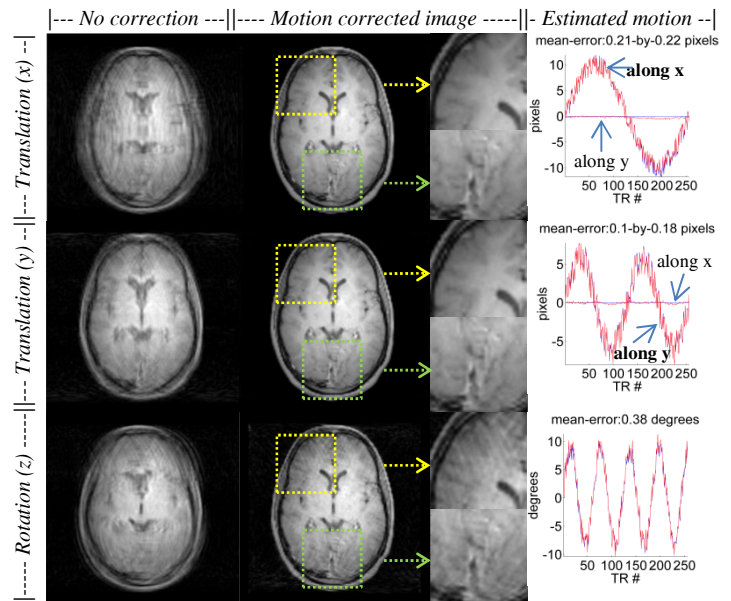


Figure 2: The proposed method is demonstrated on in-slice translational and rotational motion. **Middle column:** Parts of the corrected images are magnified to demonstrate correction performance with more clarity. **Right:** Estimated (red) and actual (blue) motion patterns are given on the right.